Canadian Conference - Pacific Conference on Earthquake Engineering 2023
Vancouver, British Columbia
June 25th – June 30th, 2023

Small Scale Model Test on the Seismic Characteristics of Floatable Building with Varied Water Height

Young-wook Lee[1], Jeongah Park[2], Gamchan Kang[3] and Gyeong-sik Kim[3]

[1]Professor, Department of Architectural Engineering, Kunsan National University, Gunsan, South Korea
[2]PhD, Researcher, Industry-University Cooperation Foundation, Kunsan National University, Gunsan, South Korea
[3]Graduated Student, Department of Architectural Engineering, Kunsan National University, Gunsan, South Korea
[*]leeyu@kunsan.ac.kr (Corresponding Author)

ABSTRACT

Earthquake-prone areas are also facing the risk of flood due to rapid climate change in recent years. Therefore, the buildings located in these areas have need to reduce risk not only of earthquakes but also of floods. To reduce these risks a floatable building can be considered. As part of a basic study on the seismic performance of these floatable buildings, this experimental study was conducted. Based on the prototype which had two floors and a basement, 1/30 scale model was made and placed in a water basin. Its base was not fixed so that it could slide if applied force was greater than frictional force. The model was also designed to behave like a rigid body in order to see the acceleration changes between the base input and the building model. The base input load was applied using one directional shaking table.

Impact and seismic loads were applied to the base of building model. The dominant period of the impact load was in short period region around 15 Hz. For the seismic load, seven ground motions matching the spectrum of S3 of the seismic design code (in Korea) were selected. From the experiments, it was shown that as the water level increased, the transmitted acceleration from the base to the building decreased. In case of the seismic load adjusted according to the similarity theory, the acceleration was reduced by about 20% when the ratio of buoyancy to building weight was 80%. As the dominant frequency of the base input acceleration was higher, the reduction of transmitted acceleration to the building was more effective.

Keywords: floatable building, earthquake, acceleration response, shaking table test, small scale model

INTRODUCTION

In recent years, extreme weather events have increased the risk of flooding due to rising sea levels and heavy rainfall. In response to this, the Buoyant Foundation Project (BFP) was launched in New Orleans in 2006 to introduce a floatable building system that installs buoyancy in the foundation. It has also been proposed to install buoyant foundations under historic buildings [1] in areas where flooding is expected to occur to enable resilient recovery from flooding. In the Netherlands, 32 floatable homes have been built in a recreational area on a dyke near Massbommel[2], and in the UK, floatable homes (see Figure 1) in a flood-prone area of Buckinghamshire have been designed to rise to the level of floodwaters.

In this study, the seismic response of a floatable building due to changes in water level was researched as part of a fundamental study for seismic design of floatable buildings. For the study, small scaled model of a building and a water tank were constructed and installed in one-directional shaking table to conduct experiments. The impact load and earthquake loads were applied to the base of the model, and the acceleration response of the model to the base input was measured by increasing the water level step by step until to floating.

CURRENT STATUS AND PRO TOTYPES

Current status

There are two main ways to achieve buoyancy in a floatable building. One is to install the buoyance body at the foundation of the building, as in the case of the BFP [1]. In this method, a buoyant body, usually made of expandable polystyrene (EPS), is installed on the lower part of the building, and lightweight steel beams are installed on top of it, and the building is placed on top of them. A mooring is installed on the outside of the building to anchor the building when floating, and a screen is installed around the foundation to prevent floating material from penetrating the lower part of the building. Another method is to use the buoyance of the building's basement, such as the example of floatables in the UK (Figure 1). The space in the concrete basement acts as a buoyant body, providing buoyancy to the building. A separate concrete walls and a slab with beams are built on the outside of the basement, and the building's basement floor is placed on top of the beams.

Previous studies of floating buildings subjected to seismic loading [3] have shown that the acceleration response of the top floor in 1/10 scale model experiments was reduced compared to the value when the foundation was fixed. However, for models in which the lateral displacement of the floating building was controlled by the mooring, the acceleration of the roof floor was sometimes greater than that of a model in which the building was fixed to the ground due to the collision of the building and the mooring under seismic loading. Therefore, it was shown that the acceleration response of a floating building could be reduced except for the collision of the building with the mooring.

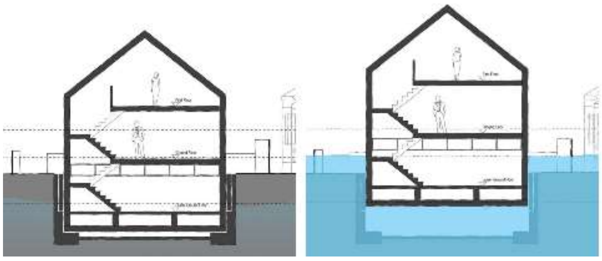

Figure 1. Floatable building with basement (https://www.baca.uk.com/amphibioushouse.html).

Table 1. Small Scale Model

Description	**Model**	
	Without Mooring	**With Mooring**
Weight (kg)	6.29	6.38
C, Center of mass from the bottom (mm)	96.8	96.8
Draft (mm)	107	107
Length x Breadth x Height (mm)	300 x 200 x 320	
Friction Coefficient	0.32	
Water tank length x breadth (mm)	357 x 260	

Prototype

As seen before, there are two types of floatable buildings: those that use buoyant materials such as EPS and those that use the buoyancy of underground structures. In this study, the buoyancy of the underground structure was selected as the prototype model.

The prototype consisted of a total of three floors, including the basement, and assumed a height of 2.7 meters for the basement, 3 meters for the first and second floors, and a plane width and length of 9 meters by 12 meters. In the prototype, the gravity load (DL+0.25LL) of the building[4] was assumed to be 3,091kN, and the model was set to float by buoyancy when the water level was above 2.9m from the bottom of the basement floor.

EXPERIMENTS

For this study, a small scale model of a floatable building and a water tank were made and shaking table experiments were conducted. The water tank was attached to the top of the one directional shaking table, the model was placed in the water tank, and input loads were applied at the base. The acceleration response of the building model was measured and analyzed by varying the water level.

Design of model

A small scale model was designed based on the prototype. The model was 1/30th the size of the prototype, with dimensions of 200mm×300mm and a total height of 320mm as in Figure 2. To make it float, the weight was adjusted using aluminum and acrylic, and the height of the basement was determined to be 120 mm to prevent the model from being submerged when floating on water.

To see clearly the acceleration changes between the base input and the building model as an initial study on the seismic design of a floatable building, the model was made as a rigid body. To behave as rigid body the lateral stiffness of it increased using aluminum plates on both sides of the model (Figure 2 (a) and Figure 3 (a)). In addition, the model with mooring was made to have a cushioning effect by using a 20mm×20mm 'L' shaped aluminum angle and sponge to prevent collision with the side wall of the tank as in Figure 3 (b). The details of the model with and without mooring is summarized in Table 1. The coefficient of friction in Table 1 is the static coefficient of friction using inclination test and is the mean value of 5 trials.

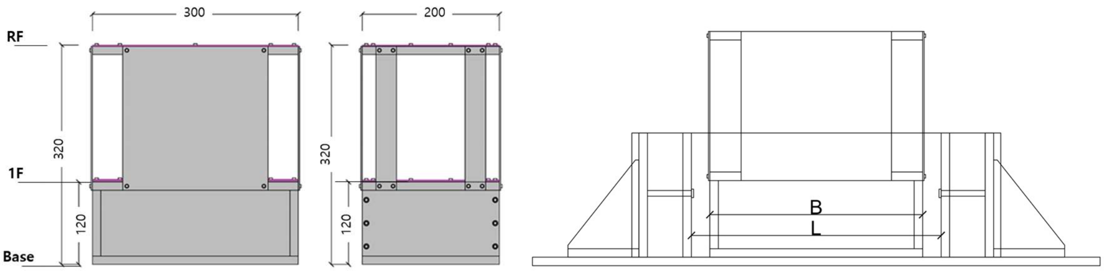

(a) *(b)* *(C)*

Figure 2. Model dimension; (a) front elevations (b) side elevations (c) building length (B) & basin length (L)

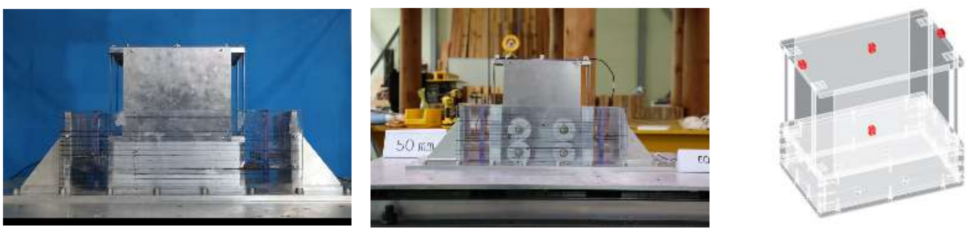

(a) *(b)* *(C)*

Figure 3. Model (a) without mooring (b) with mooring (c) measuring points for acceleration

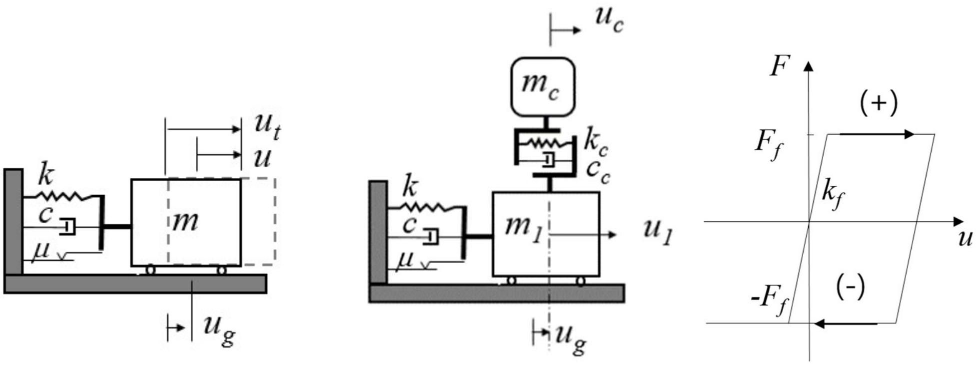

(a) *(b)* *(C)*

Figure 4. Floatable building model: (a) with no water, (b) with water, (c) friction model

Expected behavior

When there is no water in the floatable building, as shown in (a) of Figure. 4, the constitutive equations of the system [5] of building are

$$m\ddot{u} + c\dot{u} + ku + F_f = -m\ddot{u}_g(\mathrm{t}) \quad (1)$$

Where, m is the mass of building, c is the damping and k is the stiffness due to mooring, $F_f = \mu W$ is friction force, μ is the friction coefficient in the absence of water and W is the wight of building.

If there is water in the tank, as shown in (b) of Figure 4, the mass of the building can be modeled as m_1=m+m_a, where m_a is the added mass of water [5, 6]. The damping effect of the water can also be modeled as a convective mass m_c. However, since the mass of the water is relatively small compared to the mass of the building, the effect of the water may be insignificant.

If the buoyancy increases as the water level increases, the friction force will decrease, and the behavior of the building may be affected. The friction force at the water level h is shown in Eq. (2).

$$F_f = \mu(W - B) = \mu(m - hA\rho_w)\mathrm{g} \quad (2)$$

where, B is the buoyancy due to water level and A is the area of the building's basement (assuming no change in area in the basement).

In Eq. (1), when the stiffness and damping of mooring is not included, only the building mass and the friction force will be left on the left-hand side. If the inertia force of building excited by the base input acceleration exceeds the friction force, slippage occurs and the acceleration of the building is expected to decrease due to the damping effect of friction and water.

Experimental method

A water basin to control water level was constructed for this experiment and it had 356 × 260 mm in the length and width and 175 mm in height. It was made of transparent acrylic for water level control and observation of the experiment and the bottom of the tank was made of the same aluminum as the model (see Figure 2 and 3). As shown in Figure 3 (b), guides and rollers were attached to simulate mooring to keep the motion of model stable in horizontal direction when floating in the water. The rollers were 30 mm high and attached to the sides of the basin so that the model could only move in the longitudinal direction.

As in Figure 3 (c), accelerometers were attached to the center of the model to measure the horizontal acceleration of the first floor and the roof floor, and accelerometers were installed on both sides of the roof to measure the vertical acceleration to check the rocking motion.

Base input loads

Two types of base input loads were used: impact load with high-frequency rages and earthquake load with low-frequency ranges. The impact load was generated by applying 0.8 mm for 0.04 seconds. The maximum acceleration of the impact load was about 0.29g and the dominant frequency of power spectrum is about 14Hz, as in Figure 6. For the seismic loads, seven earthquake records similar to the earthquake response spectrum of soil site S_3 (Figure 5) were selected according to the seismic design standard for buildings [7]. The magnitude of the earthquakes was adjusted according to the standard to create seven EQ seismic loads as shown in Table 2. Table 2 shows the adjusted maximum acceleration of each earthquake, and the dominant frequency f_{dom} in the power spectrum of the earthquake is much lower than in the case of impact loading. The time histories and power spectra of the earthquakes are shown in Figure 7.

To see the effect of frequency of earthquake loads, the additional experiment was performed by creating seismic wave EQNs that was multiplied the time interval by $1/\sqrt{30}$ according to a similitude theory [8] but kept the acceleration at its original magnitude.

Table 2. Selected Earthquakes

ID	EQ name	Year	Max. acc. (g)	f_{dom} (Hz)
EQ1	Superstition Hills-01	1987	0.22	1.5
EQ2	Borrego Mtn	1968	0.27	1.1
EQ3	Northridge-01	1994	0.23	2.4
EQ4	Pohang	2017	0.27	1.7
EQ5	Coalinga-01	1983	0.14	1.8
EQ6	Parkfield	1966	0.25	3.6
EQ7	Mammoth Lakes-01	1980	0.32	3.4

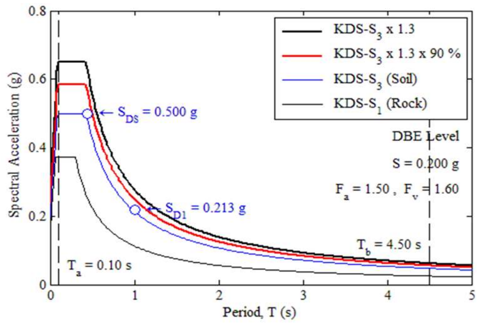

Figure 5. Earthquake response spectrum for S_3

RESULTS AND COMPARISONS

Results for impact load

The acceleration response of the first floor (herein after 1F, refer Figure 2 (a)) of the building due to the base impact load was measured with increasing water level. The maximum and minimum values and the ratio of 1F/Base acceleration are summarized in Table 3. The buoyancy ratio is the ratio of buoyancy to the building weight.

Figure 6 shows the time history and power spectrum of the acceleration of base impact load and 1F acceleration for a water level of 90 mm in the model without mooring. From the time history, it can be seen that the maximum value of 1F acceleration is reduced and delayed due to the damping effect. The dominant frequency of the power spectrum in (b) of Figure 6 occurs is 14.2 Hz for the base input acceleration and 13.8 Hz for 1F acceleration. It can be seen from the time history and spectrum that the seismic acceleration of the ground floor decreases as the building slides due to the increase in water level.

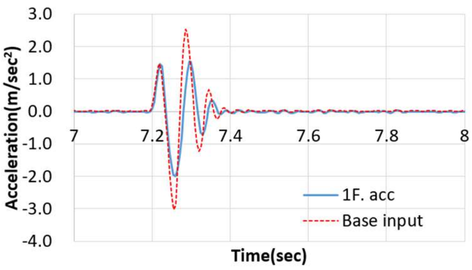

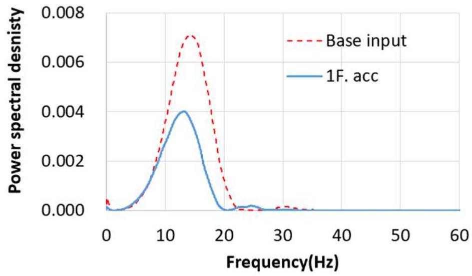

(a) *(b)*

Figure 6. Response to impact load; (a) time history (b) power spectrum

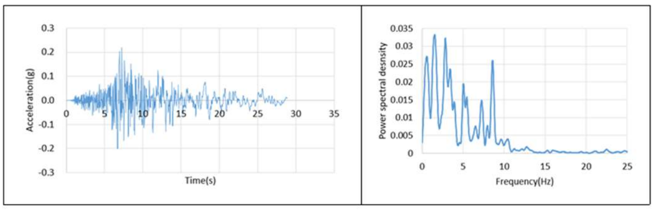

(a) EQ1

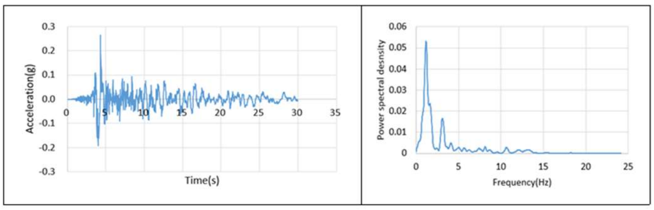

(b) EQ2

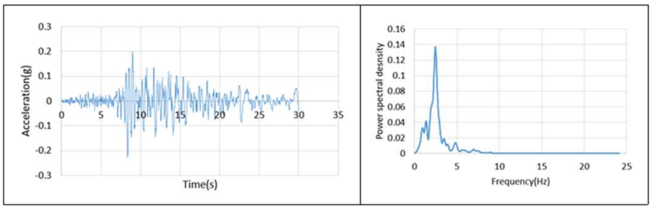

(c)EQ3

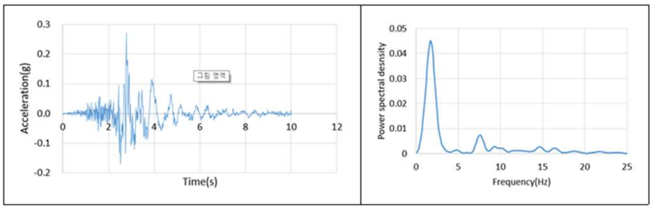

(d) EQ4

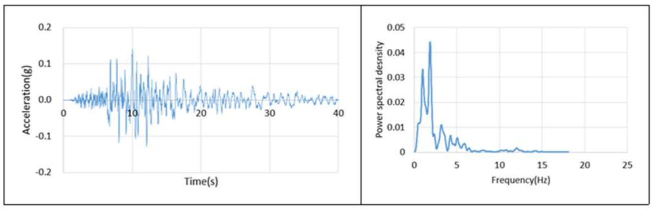

(e) EQ5

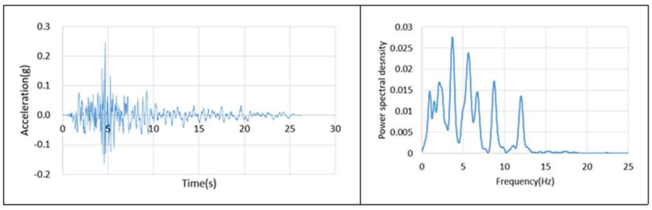

(f) EQ6

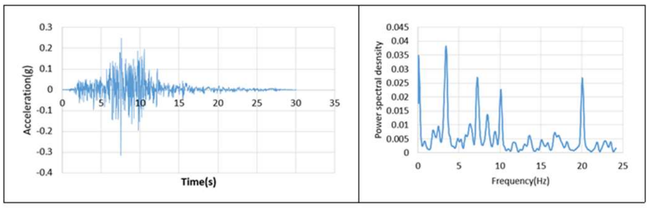

(g) EQ7

Figure 7. Time history and power spectrum for EQ loads

Table 3. Max. & Min. Accelerations of Models for Base Impact load

Buoyancy ratio (%)	Water level, (mm)	Max. & min.	Measured Acc.(m/sec^2)					
			Model without mooring			Model with mooring		
			Base	1F	ratio	Base	1F	ratio
0	0	max	2.37	2.59	1.09	1.99	2.35	1.18
		min	-2.99	-3.10	1.04	-2.87	-2.75	0.96
10	10	max	2.26	2.43	1.08	1.77	2.05	1.16
		min	-2.95	-2.91	0.99	-2.80	-2.90	1.04
29	30	max	2.16	2.39	1.11	1.90	2.17	1.14
		min	-2.83	-2.70	0.95	-2.81	-2.87	1.02
48	50	max	2.29	2.36	1.03	1.81	2.14	1.18
		min	-2.83	-2.45	0.87	-2.78	-2.59	0.93
67	70	max	2.21	2.00	0.90	1.98	2.03	1.03
		min	-2.87	-2.10	0.73	-2.80	-2.25	0.80
86	90	max	2.42	1.53	0.63	2.00	1.38	0.69
		min	-2.95	-1.89	0.64	-2.77	-1.78	0.64
100	105	max	2.21	0.77	0.35	1.85	0.69	0.37
		min	-2.77	-1.17	0.42	-2.81	-1.34	0.48

Figure 8 plots the ratio of building acceleration to the base impact load in Table 3 against the buoyancy ratio for the building weight. In both models, the ratio of building acceleration to the base input (herein after, building acceleration ratio) decreases as the water level increases, where the value with mooring being somewhat larger. In the model without mooring in Figure 8, the input acceleration and 1F acceleration are nearly to 0 for buoyancy ratios below 30%, but the building acceleration ratio gradually decreases as the buoyancy ratio exceeds 50% and the building acceleration ratio is less than 70% for buoyancy ratios above 80%.

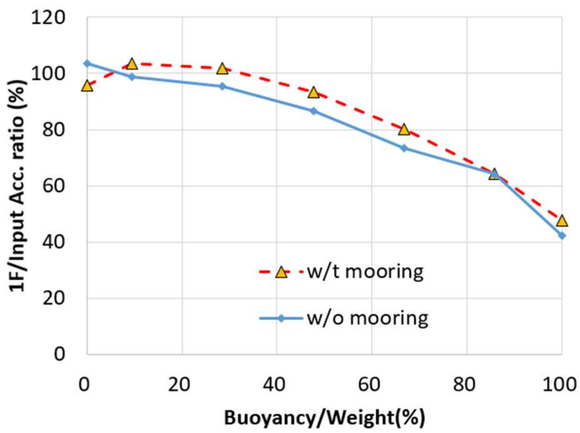

Figure 8. Relationship between 1st floor acceleration ratio with buoyancy ratio for impact load

Results for earthquake loads

The earthquake loads are applied to the model with mooring and the results are summarized in Table 4 and 5. Figure 9 (a) and (b) shows the maximum value of the building acceleration ratio to the buoyancy ratio for the earthquake load EQ and EQN. The average value for the seven earthquake loads in Figure 9 show that the building acceleration ratio tends to decrease with the increase of buoyancy ratio as in the case of impact load. In Figure 9(a), the earthquake EQ6 has the smallest building acceleration ratio, and this result may come from the components of the high frequency of the earthquake (refer Figure 7). From the average values of the EQ loads, it can be seen that the building acceleration ratio does not decrease until the buoyancy ratio of 50%, but it decreases by about 10% when the buoyancy ratio is 70% and by about 20% when the buoyancy ratio is 90%.

The graph of the experimental results for the EQN is shown in Figure 9(b). In this case, the overall trend is similar to that of the EQ case, but the building acceleration ratio is reduced relatively more. It can be seen that the reduction is about 10% at 70% buoyancy ratio and 20% at 80% buoyancy ratio. Among the seismic loads of EQN, the smallest building acceleration ratio was found in the case of EQ6N.

Table 4. Max. & Min. Accelerations for Earthquakes EQ (for Model with mooring)

Buoyancy ratio (%)	Water level (mm)	Max. & min.	Measured max. acceleration(m/sec^2) EQ1		EQ2		EQ3		EQ4		EQ5		EQ6		EQ7	
			Base	1F	Base	1F	Base	1F	Base	1F	Base	1F	Base	1F	Base	1F
0	0	max	2.24	2.35	2.69	2.70	2.20	2.25	2.28	2.38	1.73	1.74	2.87	3.02	2.11	2.21
		min	-1.63	-1.67	-2.06	-2.14	-2.36	-2.41	-1.54	-1.62	-1.54	-1.62	-2.09	-2.16	-2.31	-2.37
10	10	max	2.21	2.31	2.68	2.61	2.21	2.14	2.28	2.33	1.67	1.73	2.83	2.92	2.10	2.11
		min	-1.64	-1.66	-2.02	-2.07	-2.41	-2.44	-1.54	-1.61	-1.55	-1.55	-2.09	-2.02	-2.28	-2.38
29	30	max	2.25	2.33	2.68	2.49	2.20	2.25	2.27	2.37	1.68	1.73	2.85	2.92	2.11	2.14
		min	-1.63	-1.69	-2.02	-2.16	-2.38	-2.41	-1.53	-1.56	-1.54	-1.50	-2.07	-1.95	-2.33	-2.33
48	50	max	2.24	2.28	2.64	2.26	2.18	2.33	2.25	2.32	1.64	1.73	2.85	2.74	2.12	2.28
		min	-1.63	-1.68	-2.05	-2.17	-2.37	-2.35	-1.50	-1.58	-1.53	-1.54	-2.09	-1.99	-2.29	-2.30
67	70	max	2.23	2.18	2.78	2.54	2.20	2.20	2.33	2.37	1.68	1.73	2.90	2.66	2.09	1.61
		min	-1.64	-1.67	-2.15	-2.33	-2.34	-2.20	-1.54	-1.60	-1.55	-1.58	-2.07	-1.90	-2.29	-1.24
86	90	max	2.23	1.93	2.64	2.13	2.16	1.48	2.29	2.23	1.68	1.59	2.87	2.59	2.11	1.93
		min	-1.64	-1.70	-2.02	-1.98	-2.41	-2.03	-1.48	-1.53	-1.54	-1.44	-2.08	-1.95	-2.20	-2.13
100	105	max	2.25	1.59	2.66	1.90	2.17	1.62	2.27	1.58	1.60	1.37	2.87	2.01	2.11	1.12
		min	-1.64	-1.36	-2.02	-1.66	-2.35	-1.47	-1.48	-1.77	-1.53	-1.35	-2.05	-1.91	-2.27	-1.06

Table 5. Max. & Min. Accelerations for Earthquakes EQN (for Model with mooring)

Buoyancy ratio (%)	Water level (mm)	Max. & min.	Measured max. acceleration(m/sec^2) EQN1		EQN2		EQN3		EQN4		EQN5		EQN6		EQN7	
			Base	1F	Base	1F	Base	1F	Base	1F	Base	1F	Base	1F	Base	1F
0	0	max	1.74	1.89	–	–	2.12	2.34	2.34	2.50	1.71	1.83	3.06	3.25	2.05	2.20
		min	-2.32	-2.49	–	–	-2.21	-2.23	-2.18	-2.40	-1.32	-1.38	-2.87	-2.94	-2.33	-2.50
10	10	max	1.71	1.81	2.27	2.40	2.14	2.27	2.37	2.32	1.73	1.81	2.92	3.03	2.09	2.19
		min	-2.40	-2.51	-2.29	-2.43	-2.21	-2.20	-2.24	-2.25	-1.32	-1.37	-2.98	-2.95	-2.33	-2.46
29	30	max	1.73	1.82	2.15	2.41	2.16	2.30	2.37	2.42	1.74	1.84	3.10	3.02	2.08	2.20
		min	-2.29	-2.38	-2.25	-2.38	-2.23	-2.13	-2.15	-2.27	-1.30	-1.36	-2.87	-2.82	-2.32	-2.34
48	50	max	1.73	1.79	2.19	2.52	2.10	2.26	2.34	2.35	1.71	1.72	3.11	2.54	2.06	2.17
		min	-2.35	-2.38	-2.29	-2.35	-2.21	-1.99	-2.15	-2.22	-1.28	-1.34	-2.87	-2.65	-2.36	-2.28
67	70	max	1.79	1.65	2.23	2.37	2.17	1.99	2.34	2.01	1.73	1.58	3.05	2.21	2.09	2.13
		min	-2.32	-2.22	-2.32	-2.32	-2.24	-1.78	-2.20	-1.74	-1.28	-1.10	-2.98	-2.41	-2.32	-2.14
86	90	max	1.75	1.00	2.25	2.30	2.19	1.19	2.38	1.66	1.73	1.48	3.08	1.58	2.12	1.30
		min	-2.29	-1.30	-2.29	-2.27	-2.25	-1.47	-2.19	-1.66	-1.29	-0.88	-2.92	-1.70	-2.26	-1.77
100	105	max	1.71	0.65	2.21	1.97	2.20	0.84	2.34	0.89	1.70	0.59	2.92	1.13	2.11	0.81
		min	-2.37	-1.17	-2.27	-1.78	-2.21	-0.93	-2.18	-0.92	-1.29	-0.51	-2.95	-1.25	-2.25	-1.07

Acceleration magnitude and frequency effects

The relationship between the acceleration magnitude of the earthquakes and the building acceleration ratio as the water level changes is shown in Figure 10. Figure 10 (a) is for seven EQ loads and shows that the acceleration ratio of the building is constant regardless of the magnitude of the seismic acceleration when the water level h is 0 mm, but when h increases to 70 mm, the building acceleration ratio tends to decrease with the increase of the base acceleration. As in Figure 10 (b), the tendency for EQN loads is similar to the case of EQ but the slope of the building acceleration ratio decreases more steeply when the water level h increases to 70mm. Therefore, the building acceleration ratio tends to decrease as the buoyancy ratio (water level) increases and the magnitude of the seismic acceleration increases.

The relationship between the dominant frequency of the earthquakes and the building acceleration ratio is shown in Figure 11 as the water level changes. Figure 11 (a) is for the EQ load and shows that when h is 70 mm, the acceleration ratio of the building response tends to decrease with the increase of the frequency. Figure 11 (b) is for the EQN seismic load and has a similar shape to the EQ case, and the building acceleration ratio decreases more steeply when the water level increases to 70 mm. Therefore, it can be seen that the building acceleration ratio tends to decrease as the dominant frequency of the earthquakes increases.

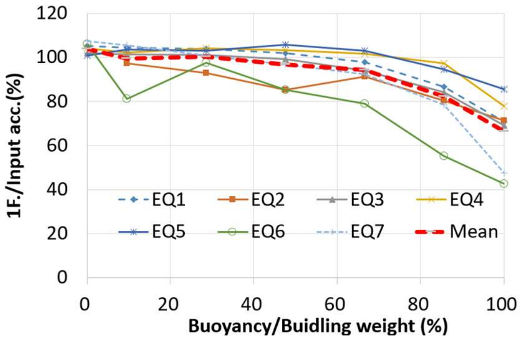

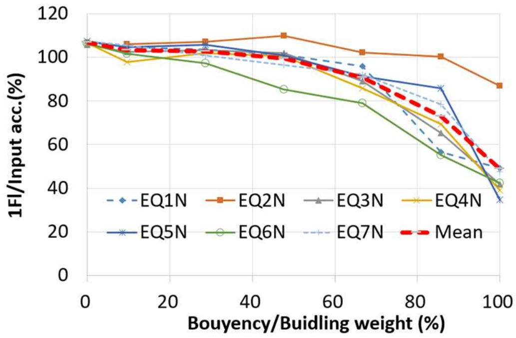

(a) *(b)*

Figure 9. Relationship between 1st floor acceleration ratio with buoyancy ratio for (a) EQ (b) EQN

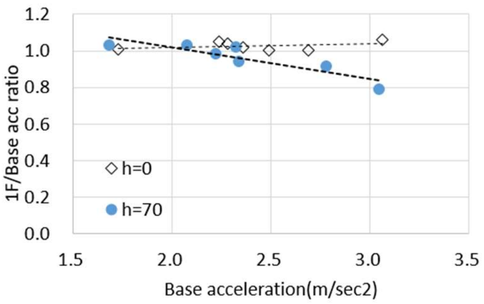

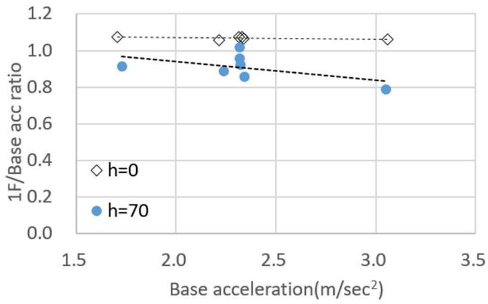

(a) *(b)*

Figure 10. Relationship between 1st floor acceleration ratio with base acceleration for (a) EQ (b) EQN

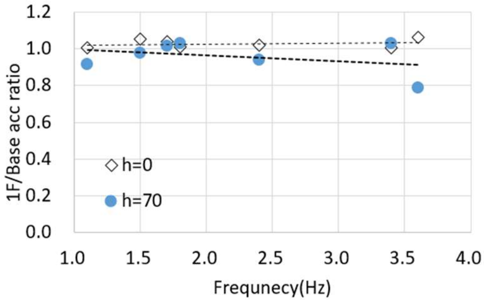

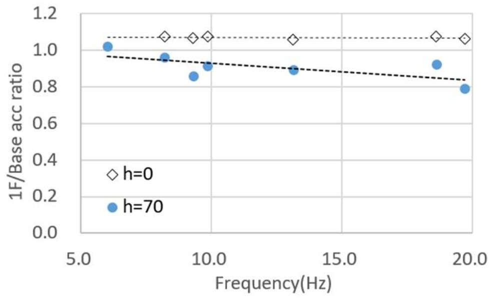

(a) *(b)*

Figure 11. Relationship between 1st floor acceleration ratio with dominant frequency of (a) EQ (b) EQN

Rocking motion effect

Because floatable systems are not anchored to the ground, but are mounted on a foundation, they can experience rocking motion as well as sliding. The vertical accelerations were measured on both sides of the roof floor to see the effect on rocking motion. The maximum acceleration with increasing water level is shown in Figure 12 for the EQ6N seismic load, where the building acceleration ratio is significantly reduced.

In Figure 12, it can be seen that the largest vertical acceleration due to rotation occurs when the water level is zero, with a maximum of 0.23m/sec^2, which corresponds to 9.4% of the maximum horizontal acceleration of 1F. However, at water levels above 10 mm, the vertical acceleration suddenly decreases. It can be said that the friction force decreases due to the water, causing slippage, which leads to a relative decrease in rocking motion. It is shown that the effect of rocking motion on the horizontal acceleration of the building is insignificant when there is water.

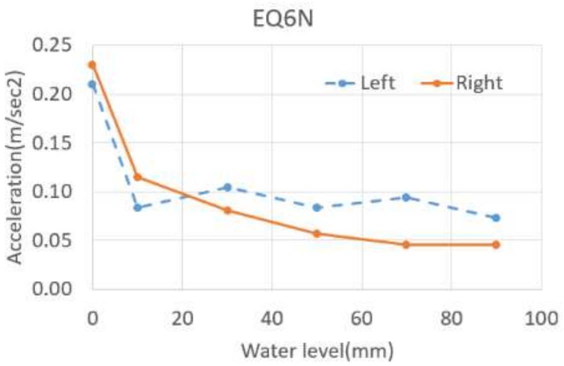

Figure 12. Vertical acceleration with water level

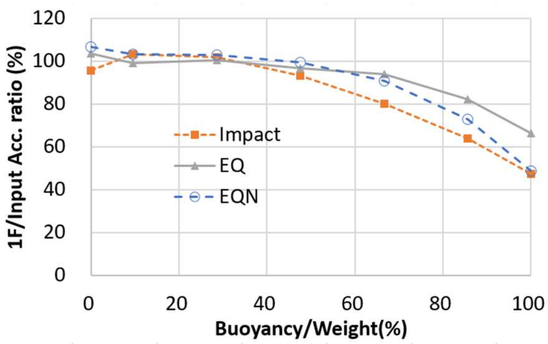

Figure 13. Comparison of results based on input load

Comparison based on input loads

For 3 types of the base inputs, the building acceleration ratio of the model with mooring is plotted against the buoyancy ratio in Figure 13. For the comparison, the mean value for earthquake load in Figure 9 are used. In Figure 13, the building acceleration ratio is the largest when the impact load is applied, followed by the average value of EQN, and then the average value of EQ.

The spectrum of the impact load (in Figure 6) has a dominant frequency of 14 Hz, while the dominant frequency of the EQ load is in the 1.1 to 3.6 Hz and the EQN is in the 6.0 to 19 Hz (Figure 11). Comparing the results of the three input loads, the building acceleration ratio is reduced the most in the case of the impact load because of the largest magnitude and the highest frequency of base input acceleration.

Comparing the average values of EQ and EQN earthquake loads in Figure 13, the building acceleration ratio of EQN decreases further as the buoyancy ratio increases above 70%. Although the magnitudes of EQ and EQN seismic accelerations are the same, the transfer of seismic loads with increasing water level decreases as the dominant frequency of earthquake shifts to the high frequency region.

CONCLUSIONS

In this paper, a small scaled model experiment was conducted to see the acceleration response of a floatable building due to an increase in water level during base ground shaking. The building model was constructed to behave as a rigid body, and a water tank was installed on a unidirectional shaking table, and the model was placed on it, and the shaking table experiments were conducted using impact loads and earthquake loads. By measuring and comparing the input ground acceleration and the response acceleration of the building as the water level increases, the following conclusions were drawn.

For both high-frequency impact loads and low-frequency earthquake loads, the acceleration ratio of the building model to the input ground acceleration decreased with an increase in the buoyancy ratio (water level). In the case of the experiments where the frequency of the earthquake was adjusted according to the similitude law, the acceleration reduction effect was insignificant in the range of 50% or less of the buoyancy ratio compared to the weight of the building, and the building acceleration ratio was reduced by 10% at 70% of the buoyancy ratio, and 20% at 80% of the buoyancy ratio.

For all three types of input base accelerations, the building acceleration ratio tended to decrease more steeply as the magnitude of the acceleration increased and as it contained more high-frequency (short period) components.

Though it was found that the acceleration response of the floatable building decreased as the buoyancy ratio increased, the reduction ratio of the acceleration transmitted to the building was as low as 10% when the buoyancy ratio was 70% or less. Therefore, further research is required on how to reduce the acceleration transmitted to the floatable building even when the building is in a low water level.

ACKNOWLEDGMENTS

This work was supported by the National Research Foundation of Korea(NRF) grant funded by the Korea government(MSIT) (NRF-2021R1A2C1009777).

This paper work was financially supported by Ministry of the Interior and Safety as Human Resource Development Project in Disaster Management.

REFERENCES

[1] English E. C., Chen M., Zarins R., Patange P. and Wiser J. C. (2019). "Building resilience through flood risk reduction: The benefits of amphibious foundation retrofits to heritage structures", *International Journal of Architectural Heritage*, https://doi.org/10.1080/15583058.2019.1695154, Taylor & Francis.

[2] Moon C.H. (2015). *Floating Architecture as a New Building Paradigm*, Floating Architecture Research (in Korean).

[3] Tsai C.S., Su H.C., Liao W.C. and Wang Y.M. (2012) "Seismic behavior of floating houses", *15th World Conference of Earthquake Engineering*. Lisboa, Portugal

[4] FEMA (2000). *Prestandard and commentary for the seismic rehabilitation of buildings*, FEMA 356.

[5] Cheng X., Jing W., Qi L. and Gong L. (2019). "Pounding dynamic responses and mitigation measures of sliding base-isolated concrete rectangular liquid storage structures", *KSCE Journal of Civil Engineering*, 23(7), 3146-3161.

[6] Housner, G. W. (1963). "The dynamic behavior of water tanks", *Bulletin of the Seismological Society of America*, 53(2), 381-387.

[7] Ministry of Land. Infrastructure and Transport (2019). *Seismic Design Standard for Buildings*, Korean Design Standard, KDS 41 17 00.

[8] Jha. A. (2004). *Dynamic Testing of Structures Using Scale Models*, A Thesis for the Degree of Master of Applied Science (Mechanical Engineering) at Concordia University, Montreal, Quebec, Canada.